

**EFFECTS OF COMBINED LOADS ON THE NONLINEAR RESPONSE AND
RESIDUAL STRENGTH OF DAMAGED STIFFENED SHELLS**

James H. Starnes, Jr. and Cheryl A. Rose
NASA Langley Research Center
Hampton, VA 23681-0001

Charles C. Rankin
Lockheed Palo Alto Research Laboratory
Palo Alto, CA 94304-1191

Presented at the FAA-NASA Symposium on Continued Airworthiness of Aircraft Structures

Atlanta, Georgia
August 28-30, 1996

EFFECTS OF COMBINED LOADS ON THE NONLINEAR RESPONSE AND RESIDUAL STRENGTH OF DAMAGED STIFFENED SHELLS

James H. Starnes, Jr. and Cheryl A. Rose
NASA Langley Research Center
Hampton, VA 23681-0001

Charles C. Rankin
Lockheed Palo Alto Research Laboratory
Palo Alto, CA 94304-1191

ABSTRACT

The results of an analytical study of the nonlinear response of stiffened fuselage shells with long cracks are presented. The shells are modeled with a hierarchical modeling strategy and analyzed with a nonlinear shell analysis code that maintains the shell in a nonlinear equilibrium state while the crack is grown. The analysis accurately accounts for global and local structural response phenomena. Results are presented for various combinations of internal pressure and mechanical loads, and the effects of crack orientation on the shell response are described. The effects of combined loading conditions and the effects of varying structural parameters on the stress-intensity factors associated with a crack are presented.

INTRODUCTION

Transport fuselage shell structures are designed to support combinations of internal pressure and mechanical flight loads which can cause a geometrically nonlinear structural response. These fuselage shell structures are required to have adequate structural integrity so that they do not fail if cracks occur in service. The structural response of a stiffened fuselage shell structure with one or more cracks is influenced by the local stress and displacement gradients near the cracks and by the internal load distribution in the shell. Local displacements near a crack can be large compared to the fuselage skin thickness, and these displacements can couple with internal stress resultants in the shell to amplify the magnitudes of the local stresses and displacements near the crack. This nonlinear response must be understood and accurately predicted in order to determine the structural integrity and residual strength of a fuselage structure.

Recent studies (e.g., Refs. 1-3) have shown that the stiffness and internal load distributions in a stiffened fuselage shell will change as a long crack grows in the shell. These changes affect the local stress and displacement gradients near the crack in a manner that may contribute to additional crack growth in the shell and, as a result, affect its structural integrity and residual strength. Refs. 1-3 show that the structural response and structural integrity of a stiffened fuselage shell with a crack can be studied analytically using a nonlinear structural analysis procedure that models crack growth in the shell. Results from a nonlinear analysis procedure more accurately represent the local and global responses of a thin stiffened shell with a crack than the results from a conventional linear analysis procedure for all loading conditions.

The present paper describes the results of an analytical study of the nonlinear response of a typical stiffened fuselage shell structure with long cracks and subjected to various combinations of

internal pressure and mechanical loads. Both longitudinal and circumferential fuselage cracks are considered. The results illustrate the influence of the different loading conditions on the local stress and displacement gradients near a crack, on the magnitudes of the stress-intensity factors associated with the crack, and on crack-growth trajectories. The effects of varying structural parameters, such as fail-safe-strap thickness and stiffener area, and varying crack orientation on the results are described. The effects of loading conditions and crack location relative to stiffening members on both self-similar and non-self-similar crack-growth trajectories are also presented.

NONLINEAR ANALYSIS PROCEDURE AND HIERARCHICAL MODELING STRATEGY

A nonlinear shell analysis procedure that is combined with a hierarchical modeling strategy is used in the present study to analyze the nonlinear response of a typical stiffened fuselage shell with long skin cracks. The analysis procedure models crack growth in a shell while the shell is in a nonlinear equilibrium state, and determines local stress and displacement gradients in critical areas of a fuselage where cracks may be growing. In addition, the analysis procedure accurately models frame and stringer cross-sectional distortion and rolling, and predicts the nonlinear interactions that occur between individual structural elements and larger subcomponents as a result of these deformations. The details of the analysis procedure and modeling strategy are discussed subsequently.

Nonlinear Analysis Procedure

The STAGS (S_TStructural Analysis of General Shells) nonlinear finite element analysis code⁴ is used in the present study to conduct the nonlinear analyses of stiffened fuselage shells with long cracks. STAGS is a finite element code for analyzing general shell structures and includes the effects of geometric and material nonlinearities in the analysis. STAGS is capable of conducting strength, stability and collapse analyses for general shell structures with complex geometry and subjected to combined mechanical and thermal loads. The code uses both the modified and full Newton methods for its nonlinear solution algorithms, and accounts for large rotations in a shell by using a co-rotational algorithm at the element level. STAGS has static and transient analysis capabilities that can be used to predict local instabilities and modal interactions that occur due to destabilizing mechanical loads, such as an applied compression or shear load. The Riks pseudo arc-length path following method⁵ is used to continue a solution past the limit points of a nonlinear response. A boundary constraint function, based on a least-squares analysis, is used to apply equivalent beam loads to the boundary of a thin-shell finite element model without artificially distorting the shell wall. By using this least-squares constraint function, flight loads can be extracted from a lower fidelity global aircraft model and then applied as edge loads on the boundaries of a more refined finite element model of a fuselage shell section.

STAGS can also perform crack-propagation analyses. Cracks in simple unstiffened shells and in built up structures and structural elements, such as frames, stringers and fail-safe straps, can be modeled. A node-release method and a load-relaxation technique are used to extend a crack while the shell is in a nonlinear equilibrium state.² The forces necessary to hold the nodes together along the path of new crack growth are calculated with this method. These forces are relaxed as the crack is extended, and a new equilibrium state is calculated which corresponds to the longer crack. The changes in the stiffness matrix and the internal load distribution that occur during crack growth are accounted for in the analysis, and the nonlinear coupling between internal forces and in-plane and out-of-plane displacement gradients that occurs in a shell are properly represented. Output from STAGS includes strain-energy-release rates that can be used to determine stress-intensity factors. The stress-intensity factors^{2,6} can then be used to estimate the residual strength of a damaged shell.

The FRANC3D (FRacture ANalysis Code for 3D surfaces) fracture analysis code⁷ has been interfaced with STAGS to predict curved or non-self-similar crack-growth trajectories. STAGS results are transmitted to FRANC3D which computes the stress intensity factors at the crack tips using the modified crack closure integral method, and an estimate of the crack growth direction at each tip is computed by applying the maximum tangential stress criterion. Using these parameters, the crack is grown within FRANC3D by a user specified length. After the crack is grown, FRANC3D creates a new finite element mesh in the area of the crack. The STAGS results from the previous finite element mesh are mapped onto the new finite element mesh using a transformation subroutine that is compatible with STAGS. The nonlinear STAGS analysis can then be continued with the new finite element mesh results from FRANC3D.

Hierarchical Modeling Strategy

A hierarchical modeling strategy is used in the present study for the analysis of stiffened fuselage shell sections subjected to combined internal pressure and mechanical loads. The three hierarchical modeling levels used to obtain the analysis results presented in this paper are characterized by a global shell model, a 6x6 bay stiffened-panel model, and a 2x3 bay stiffened-panel model. Different modeling idealizations are employed in the three levels in the hierarchy.

The first level in the hierarchical modeling strategy uses a global stiffened fuselage shell model that is subjected to combined internal pressure and mechanical loads. The mechanical loads are applied as concentrated loads to one end of the global fuselage shell model using a least squares boundary constraint function. Symmetry conditions are imposed at the other end. The global stiffened shell model includes floor beams and stanchions, frames, stringers, fail-safe straps, and stringer clips. The skin is modeled with shell elements; the frames, which may have non-symmetric cross sections, are modeled with shell and beam elements, in order to represent accurately the cross-sectional bending and twisting of the frames; and the floor beams, stanchions, fail-safe straps, stringers, and stringer clips are modeled with beam elements. Damage is introduced in the global model in the form of longitudinal or circumferential skin cracks and may also include broken frames, stringers and fail-safe straps. A geometrically nonlinear analysis of the global shell model provides the internal load distribution for the fuselage shell and kinematic boundary conditions for the 6x6 bay stiffened-panel model.

The 6x6 bay stiffened-panel model has a higher degree of mesh refinement and structural detail than the global model described above in order to represent more accurately the structural response around the crack, and the distortion of the frames and stringers. Frames, stringers, and stringer clips are modeled as branched shells in the 6x6 bay stiffened-panel model, and the fail-safe straps are modeled using shell elements. In addition, the mesh is sufficiently refined around the crack tip for calculating crack-growth parameters.

Displacements obtained from the 6x6 bay stiffened-panel model are used as boundary conditions for the third modeling level, which consists of a more detailed, highly local 2x3 bay stiffened-panel model. The 2x3 bay stiffened-panel model differs from the 6x6 bay stiffened-panel model primarily in the degree of mesh refinement, and may also include additional structural details such as lap joints and fasteners. The fasteners are modeled in STAGS with nonlinear spring elements. In addition, at this modeling level, the STAGS analysis is interfaced with FRANC3D to simulate general, curved, non-self-similar crack growth trajectories. Results from a nonlinear STAGS analysis of the original structural configuration are mapped into FRANC3D where the modified crack closure integral method is used to determine stress intensity factors at each crack tip and an estimate of the crack growth direction at each tip is computed by applying the maximum tangential stress criterion.⁷ Using these parameters, the crack is extended within FRANC3D, by an amount specified by the analyst, and the 2x3 bay model is remeshed in the area of the crack. The STAGS results from the previous finite element mesh are mapped onto the new finite element mesh. The new mesh is then

employed for the next STAGS analysis. The steps described above are repeated to obtain a crack trajectory and stress intensity factor history.

Generic Narrow-Body Transport Fuselage Model

The fuselage shell analyzed in this study is a typical generic narrow-body transport aluminum fuselage. The shell has a 74-inch radius and is 160 inches long. The shell consists of 0.036-inch-thick 2024-T3 clad aluminum skin, and is reinforced by nine frames that are spaced 20 inches apart and fifty stringers that are spaced 9.3 inches apart. The stringers and frames are made of 7075-T6 aluminum. Fail-safe straps are located beneath each frame and stringer, and additional circumferential fail-safe straps are located midway between frames. The fail-safe straps are 0.036 inches thick, the stringers are 0.028 inches thick hat sections, and the frames are 0.040 inches thick Z-sections, unless otherwise noted. A Poisson's ratio equal to 0.33 is used for all structural components, a Young's modulus equal to $10.5E6$ psi is used for the skin and tear straps and a Young's modulus equal to $10.7E6$ psi is used for the frames, stringers and stringer clips in all analyses. In addition, it is assumed that a perfect bond exists between all structural components along their entire area of overlap, at all modeling levels. Circumferential and longitudinal cracks are located in the crown, midway between the ends of the global fuselage shell model.

The loads considered in the present study include internal pressure, up and down bending, vertical shear, and torsion. The internal pressure is equal to 8 psi for all analyses which is the nominal operating pressure in the passenger cabin of a typical subsonic transport. Tensile axial stress resultants are applied to the model to represent the loads from the pressure bulkheads. The magnitudes of the bending and vertical shear loads used in this study are the maximum values of these applied loads that can be supported by an undamaged global shell model without buckling the skin. The applied bending moment is equal to 6,325,000 in-lbs, and the applied shear force is equal to 50,000 lbs., unless otherwise noted. Up-bending moments are applied to the model with a longitudinal crown crack so that the crack is loaded in compression. Axial compression has been shown³ to cause higher stress-intensity factors at the tips of longitudinal crown cracks than are caused by axial tension. Both up- and down-bending moments are applied to the global models with a circumferential crack so that the fuselage crown is loaded in either compression or tension, respectively.

RESULTS AND DISCUSSION

Results of the stiffened fuselage nonlinear analysis have been generated for seven loading conditions: internal pressure plus a bending load; internal pressure plus a vertical shear load; internal pressure plus a torsion load; internal pressure plus bending and torsion loads; internal pressure plus bending and vertical shear loads; internal pressure plus vertical shear and torsion loads; and internal pressure plus bending, vertical shear and torsion loads. Results for these loadings are presented for both longitudinal and circumferential cracks to illustrate the effects of crack orientation and the applied loading condition on the structural response.

Results are presented in the form of stress-intensity factor versus crack-length plots, stress resultant contours and deformed shape plots, and crack growth trajectories. The stress-intensity factors presented were obtained from the 6x6 bay stiffened-panel models. To simulate crack growth in the 6x6 bay stiffened-panel models, the longitudinal cracks were grown from an initial length of 6.0 inches to a final length of 18.5 inches, and the circumferential cracks were grown from an initial length of 4.7 inches to a final length of 17.7 inches. Boundary conditions for the 6x6 bay stiffened-panel models with a longitudinal crack or a circumferential crack were obtained from a global model with a 6.0-inch-long longitudinal crack or a 4.7-inch-long circumferential crack, respectively. Crack-growth

trajectories for a longitudinal crack were obtained using a 2x3 bay stiffened-panel model with an initial crack length of 6.0 inches. Boundary conditions for the 2x3 bay model were obtained from the 6x6 bay stiffened-panel model with a 6-inch-long crack.

6x6 Bay Stiffened Panels with a Longitudinal Crack

The stress-intensity factors K_I and K_{II} , which correspond to a crack-opening mode and a crack-shearing mode, are shown in figures 1a and 1b, respectively, as a function of longitudinal crack length, for the seven combined loading conditions considered in this study. The legend in the figures identifies the loading conditions by combinations of the letters P, M, S and T, which indicate the internal pressure, bending, vertical shear, and torsion loads, respectively. The solid lines represent results for internal pressure plus one mechanical load component, and the dashed lines represent results for internal pressure plus more than one mechanical load component. As shown in figure 1a, the loading conditions with bending (M) and vertical shear (S) have higher values of K_I than those with torsion (T). This trend is explained by the fact that in the bending and vertical shear loading cases, high axial compressive stresses are present in the crown panel that couple with the out-of-plane displacements along the edges of the crack. The loading conditions with torsion have high values of shear stress resultants in the crown panel and are not represented by a simple crack-opening response. Consequently, the panels subjected to torsion loading have higher values of K_{II} than those without a torsion load, as shown in figure 1b. In addition, the curves representing the change in K_I as the crack length increases in figure 1a are not linear, and the slope of the curves decreases as the crack length increases. The curves for K_{II} are mildly nonlinear. The decrease in slope of the K_I curves with increasing crack length is explained by noting that as the crack length increases, the loads in the skin are redistributed to the frames and fail-safe straps, and the cross-sections of the stringers on either side of the crack distort enough to reduce the stiffnesses of the stringer.

Values of the stress-intensity factors are typically used to determine the residual strength of a stiffened shell structure as a crack grows. An example residual strength diagram for a stiffened shell with a longitudinal crack in the skin and a broken frame, and subjected to pressure loading, is shown in figure 2. The diagram shows a skin fracture curve, plotted as a solid line, and a frame yield curve for the next intact frame, plotted as a dotted line. The solid curve is a plot of the critical far-field hoop stress in the skin as a function of crack length. The critical far-field hoop stress is determined from the pressure that would cause the dominant crack-tip stress-intensity factor to become critical for each crack length. The curve for the frame is determined from the far-field hoop stresses that correspond to yielding in the frame for each crack length. In general, the curves in figure 2 indicate that the residual strength of the skin and the frame decreases as the crack grows. The residual strength of the skin decreases significantly as first, and then increases slightly as the crack approaches a fail-safe strap because some of the skin load is redistributed to the fail-safe strap. The residual strength of the frame decreases once the crack has grown past the fail-safe strap because some of the skin load is redistributed to the frame, which causes the frame to yield at a lower load. The crack in the skin will grow before the frame yields if the residual strength of the skin is less than the residual strength of the frame. In contrast, the frame will yield before the skin crack grows when the residual strength of the frame is less than the residual strength of the skin. The structure has no residual strength when the two curves have values less than prescribed allowable strength values.

The effects of varying fail-safe-strap thickness, t , on the stress-intensity factor K_I for a panel with a longitudinal crack and subjected to internal pressure and a bending or a torsion load are shown in figure 3. Fail-safe-strap thicknesses equal to 0.018, 0.036 and 0.054 inches were used. The solid curves are for internal pressure and bending loads and the dashed curves are for internal pressure and torsion load. The length of the crack varies from 6.0 to 18.5 inches. The results presented in figure 3 indicate that K_I increases as the fail-safe-strap thickness decreases. In addition, as previously shown in figure 1, the loading with bending produces higher values of K_I than the corresponding loading in

torsion. Moreover, the slope of the K_I curves decreases as the crack approaches the frames and the load in the skin is redistributed to the frames. The decrease in the slope of the K_I curves is more significant for the loading with bending. Similar results from the analysis for K_{II} indicate that K_{II} is not significantly affected by these changes in the fail-safe-strap thickness; however, there is a slight increase in K_{II} as the fail-safe strap thickness decreases.

6x6 Bay Stiffened-Panels with a Circumferential Crack

Stress resultant distribution contour plots obtained from the nonlinear analyses of a 6x6 bay stiffened-panel with an 17.7-inch-long circumferential crack are shown on the corresponding deformed shapes in figures 4 and 5 for a stiffened panel subjected to combinations of internal pressure and bending loads, and a stiffened panel subjected to internal pressure and torsion, respectively.

In a panel subjected to internal pressure only (not shown) the edges of the crack spread apart and the crack opens. The material line elements along the edges of the crack are in hoop tension because of the outward bulging deformations in the local crack region that are caused by the internal pressure. The outward bulging deformations near the crack are not symmetric for this crack location because the crack has a relatively stiff frame on one side and a relatively flexible fail-safe strap on the other side. The hoop stress resultant distribution results in a panel that is subjected to internal pressure and a down-bending moment are shown in figure 4a. This loading condition also causes the edges of the crack to spread apart and open the crack, but the skin along the edges of the crack is in hoop compression except at the crack tips where a significant tensile stress resultant exists. Apparently, the compressive hoop stress resultant induced by the tensile axial stress resultant caused by the down-bending moment is large enough to dominate the tensile hoop stress resultant along the edge of the crack caused by the internal pressure. The down-bending moment causes a significant tensile axial stress resultant gradient near the crack, as shown in figure 4b, and a biaxial tension stress state exists at the crack tip for this loading condition. In a panel that is subjected to internal pressure and an up-bending moment, compressive axial stresses in the crown, resulting from the up-bending moment, cause the edges of the crack to approach one another and contact occurs at several locations (not shown). One edge of the crack contacts the webs of the broken stringer on the other edge of the crack, and the two edges of the crack contact each other at two other locations. The contact was not accounted for in the analysis, and will be considered in future analyses. The skin along the edges of the crack is in hoop tension for this loading condition along the entire length of both crack edges. Apparently, the tensile hoop stress resultant induced by the compressive axial stress resultant caused by the up-bending moment increases the magnitude of the tensile hoop stress resultant along the edges of the crack caused by the internal pressure.

The axial stress resultant distribution results in a panel with a 17.7-inch-long circumferential crack and subjected to internal pressure and torsion loads are shown in figure 5a. The crown is primarily in axial tension because of the tension load induced by the pressure bulkhead. The outward bulging deformations near the crack are not the same on both sides of the crack for this loading condition, and the edges of the crack are displaced circumferentially or sheared relative to one another and significantly distorted. Therefore, the local displacements of the crack are not representative of a simple crack-opening mode. The hoop stress resultant distribution for this loading condition is shown in figure 5b and does not have reflective symmetry, due to the torsion load. The results indicate that the hoop stress resultant in the skin at the crack tips has a relatively high tensile value for this loading condition.

The stress-intensity factors K_I and K_{II} , are shown as a function of circumferential crack length in figures 6a and 6b, respectively, for the seven combined loading conditions considered in this study. The legend convention used in figure 1 is also used in figure 6. One half of the values of the moment and vertical shear loads previously stated were used in the analysis for the loading conditions with both

the bending (M) and vertical shear loads (S) to prevent the crack faces from contacting. The loading condition with internal pressure and a torsion load has the highest value of K_I , and all loading conditions with a torsion load have high values of K_{II} . For a torsion load only, there is no axial compression to close the crack which would cause a higher value of K_I . The torsion load causes one crack face to deform more than the other, which causes a higher value of K_{II} . The bending and vertical shear loads cause the crack to close which, reduces the value of K_I . The curves representing the change in K_I and K_{II} as a function of crack length in figures 6a and 6b are not linear as the crack length increases because of the internal load redistribution that occurs. The redistribution of internal loads changes the stress magnitudes in the skin, and, as a result, changes the magnitudes of the stress-intensity factors.

The effects of varying the stringer cross-sectional area on the stress-intensity factor K_I for a panel with a circumferential crack and that is subjected to internal pressure and torsion are shown in figure 7. The area of the stringer is varied by changing the thickness, t , of all components of the stringer hat section. The results in the figures are for thicknesses, t , equal to 0.028, 0.036 and 0.040 inches. The length of the crack varies from 4.7 to 17.7 inches. The results in figure 7 indicate that K_I increases as the stringer area decreases and as the crack length increases, which suggests that the skin has higher axial stress resultants when the stringer is thinner. The results from the analysis indicate that K_{II} increases as the stringer thickness decreases for all crack lengths, which suggests that thicker stringers restrain the shear deformations near the crack and reduce the shear stress resultants in the skin. The values of K_I and K_{II} both decrease as the crack length increases beyond approximately 15.0 inches because the crack tips are approaching the stringers on either side of the broken stringer and the load in the skin is redistributed to the intact stringers.

Crack-Growth Trajectories

The effects of loading condition and crack location on crack growth trajectories were studied using a detailed 2x3 bay local-panel model that is centered around the crack. Displacements obtained from the 6x6 bay stiffened-panel model with a 6-inch-long longitudinal crack were applied as boundary conditions for the 2x3 bay local-panel model. Crack-growth trajectories are shown in figure 8 for three longitudinal crack locations and loading conditions. The initial crack length for these longitudinal crack configurations is 6.0 inches, and the crack is located either midway between two stringers or 1.2 inches from a stringer. The crack-growth trajectory for a crack located midway between two stringers in a panel that is subjected to internal pressure, bending and vertical shear loads is shown in figure 8a for a crack length of 16.0 inches. The crack-growth trajectory for this case is self-similar due to the symmetry of the loading condition and geometry. The crack-growth trajectory for a crack located 1.2 inches from a stringer in a panel subjected to internal pressure, bending and vertical shear loads is shown in figure 8b for a crack length of 16.0 inches. The crack-growth trajectory for this case is non-self-similar due to the asymmetry of the geometry. The crack-growth trajectory for a crack that is located midway between two stringers in a panel that is subjected to internal pressure and torsion shear loads is shown in figure 8c for a crack length of 16.0 inches. The crack-growth trajectory for this case is non-self-similar due to the nonsymmetry of the loading condition.

CONCLUDING REMARKS

The results of an analytical study of the effects of long cracks on the nonlinear response of stiffened fuselage shells subjected to combined internal pressure and mechanical loads are presented. The nonlinear analysis predicts the large local stress and out-of-plane displacement gradients that exist

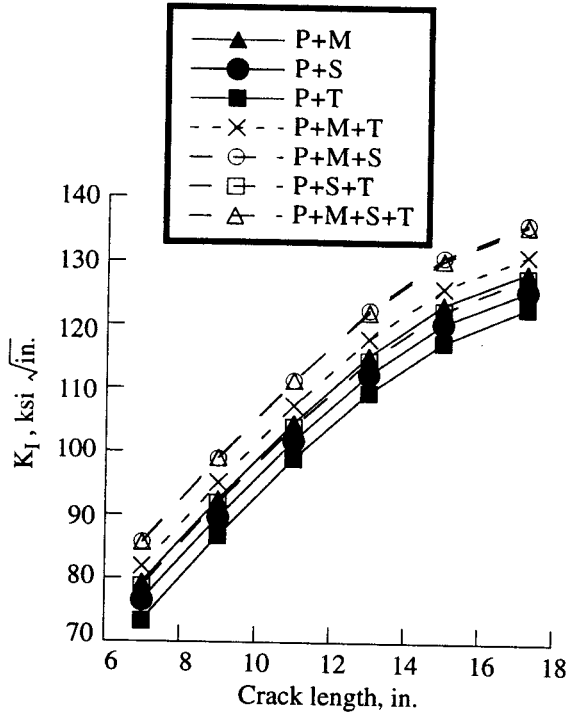
near cracks in stiffened shells, and accounts for the coupling that occurs between the in-plane stress resultants and the out-of-plane displacements in the neighborhood of the crack.

The results of the nonlinear analyses show that the response of a damaged stiffened shell subjected to combined internal pressure and mechanical loads is affected by both the load combination and the crack orientation. In the case of a longitudinal crown crack, the axial compressive stresses in the crown that are caused by bending and vertical shear loads can couple with the out-of-plane displacements in the crack region to amplify the magnitudes of the local stresses and displacements, thereby increasing the crack-opening stress-intensity factor. On the other hand, compressive axial stress resultants can close a circumferential crack and reduce the crack-opening stress-intensity factor associated with the crack. Tensile axial stress resultants can open a circumferential crack. Torsion loads can also significantly affect the local response of a shell with a circumferential crack by causing the edges of the crack to shear relative to one another and by increasing the crack-shearing stress-intensity factor associated with the crack.

As a crack grows in a stiffened shell, the internal loads are redistributed from the fuselage skin to other structural elements, such as frames, stringers and fail-safe straps, and this internal load redistribution affects the magnitudes of the stress-intensity factors associated with a crack. Varying the thickness of the fail-safe straps or the area of the stringers can affect the magnitudes of the stress-intensity factors, which will affect residual strength. The crack-growth trajectory can be influenced by the crack location and by the loading condition. Nonsymmetric loading conditions or geometries can cause non-self-similar crack-growth trajectories.

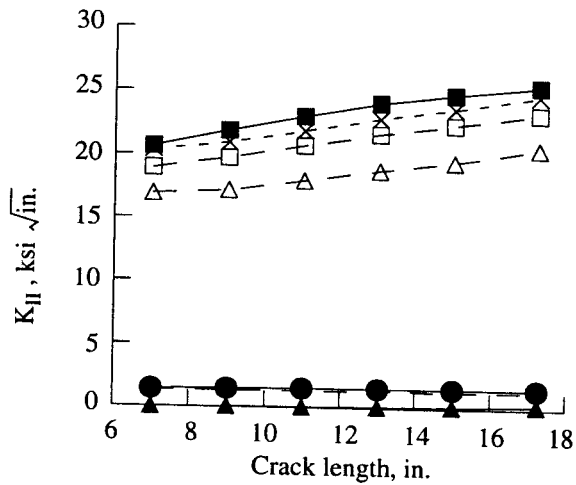
REFERENCES

1. Riks, E.: *Bulging Cracks in Pressurized Fuselages: A Numerical Study*. NLR MP 87058 U, NLR National Aerospace Laboratory, The Netherlands, September 1987.
2. Rankin, C. C., Brogan, F. A., and Riks, E.: *Some Computational Tools for the Analysis of Through Cracks in Stiffened Fuselage Shells*. *Computational Mechanics*, Springer International, Vol. 13, No. 3, December 1993, pp. 143-156.
3. Starnes, James H., Jr., Britt, Vicki O., and Rankin, Charles C.: *Nonlinear Response of Damaged Stiffened Shells Subjected to Combined Internal Pressure and Mechanical Loads*. AIAA Paper 95-1462, April 1995.
4. Brogan, F. A., Rankin, C. C., and Cabiness, H. D.: *STAGS User Manual*. Lockheed Palo Alto Research Laboratory, Report LMSC P032594, 1994.
5. Riks, E.: *Some Computational Aspects of the Stability Analysis of Nonlinear Structures*. *Computational Methods in Applied Mechanics and Engineering*, Vol. 47, pp. 219-259, 1984.
6. Riks, E., Brogan, F. A., Rankin, C. C.: *Bulging of Cracks in Pressurized Fuselages: A Procedure for Computation*. in *Analytical and Computational Models of Shells*, Noor, A. K., Belytschko, T., and Simo, J. C., Editors, The American Society of Mechanical Engineers, ASME-CED Vol. 3, 1989.
7. Potyondy, D. O. *A Software Framework for Simulating Curvilinear Crack Growth in Pressurized Thin Shells*. PhD Dissertation, Cornell University, Ithaca, NY, 1993.



(a) K_I stress-intensity factor.

Fig. 1 Stress-intensity factors for a six-bay by six-bay stiffened fuselage crown panel with an 18.5-inch-long longitudinal crack subjected to internal pressure and mechanical loads.



(b) K_{II} stress-intensity factor.

Fig. 1 Concluded.

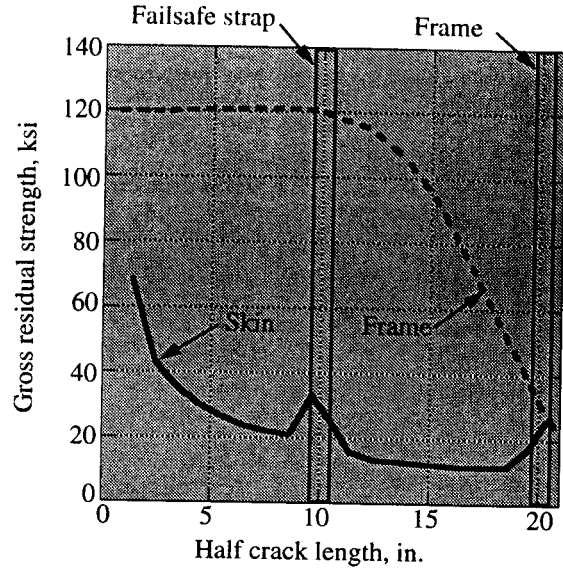


Fig. 2 Residual strength of a stiffened fuselage crown panel with a longitudinal skin crack and broken frame, and subjected to internal pressure.

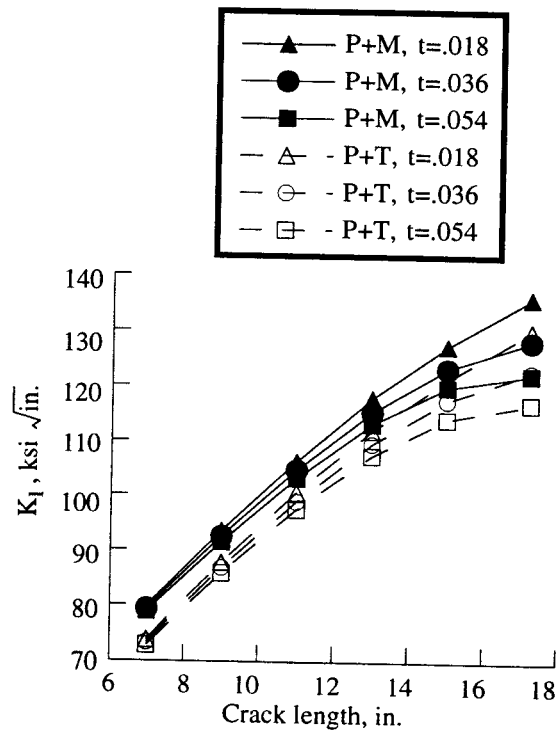
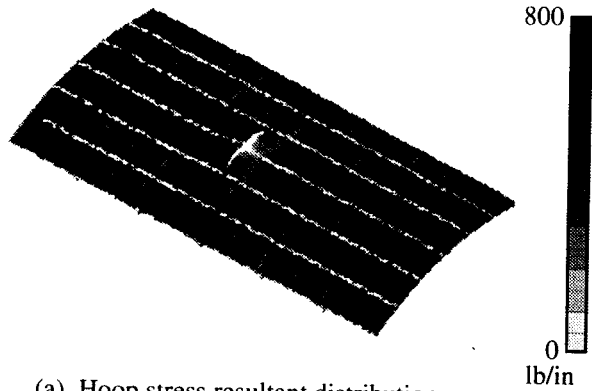
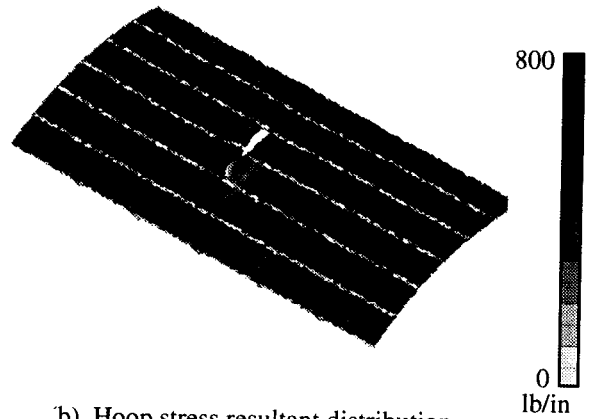


Fig. 3 Effects of varying fail-safe-strap thickness on the K_I stress-intensity factor for a six-bay by six-bay stiffened fuselage crown panel with an 18.5-inch-long longitudinal crack and subjected to internal pressure, bending and torsion loads.



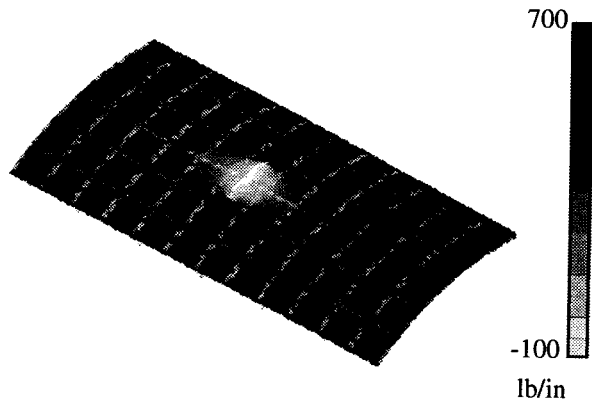
(a) Hoop stress resultant distribution.

Fig. 4 Stress resultant distributions in a six-bay by six-bay stiffened fuselage crown panel with a 17.7-inch-long circumferential crack and subjected to internal pressure and down-bending loads.



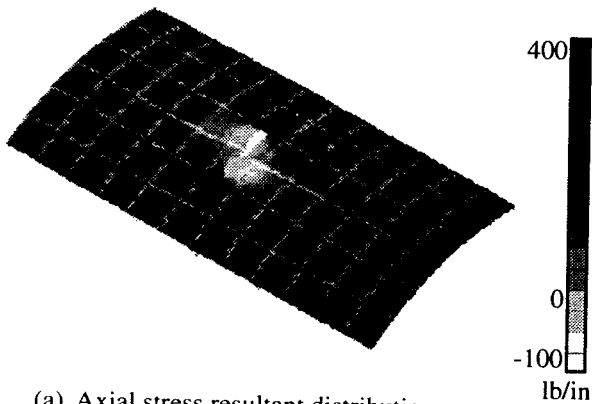
(b) Hoop stress resultant distribution.

Fig. 5 Concluded.



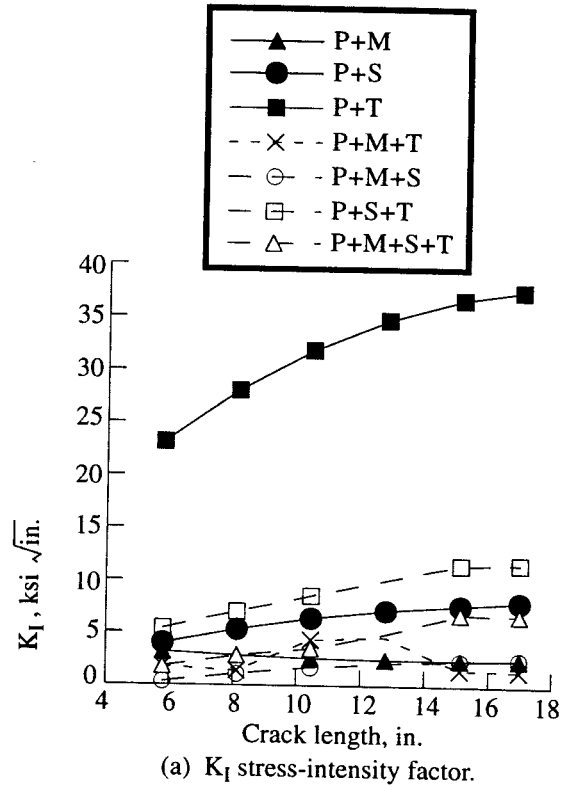
(b) Axial stress resultant distribution.

Fig. 4 Concluded.



(a) Axial stress resultant distribution.

Fig. 5 Stress resultant distributions in a six-bay by six-bay stiffened fuselage crown panel with a 17.7-inch-long circumferential crack and subjected to internal pressure and torsion loads.



(a) K_I stress-intensity factor.

Fig. 6 Stress-intensity factors for a six-bay by six-bay fuselage crown panel with an 17.7-inch-long circumferential crack and subjected to internal pressure and mechanical loads.

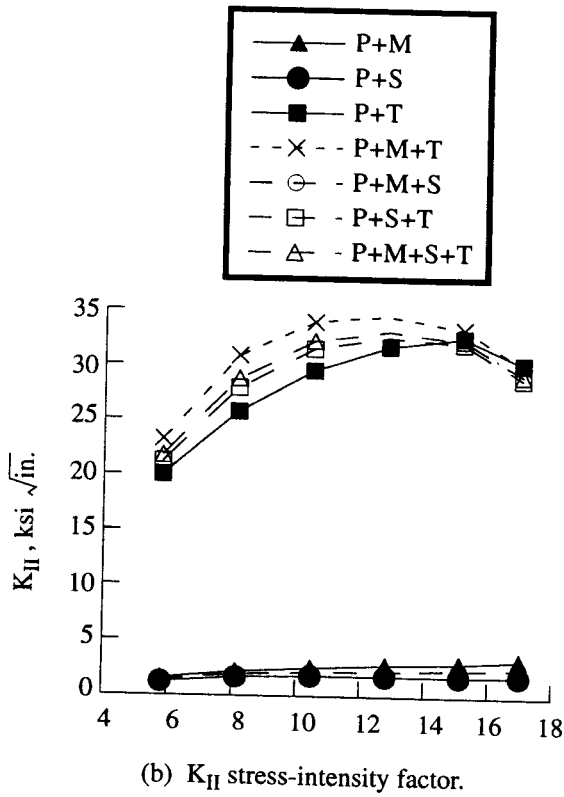


Fig.6 Concluded.

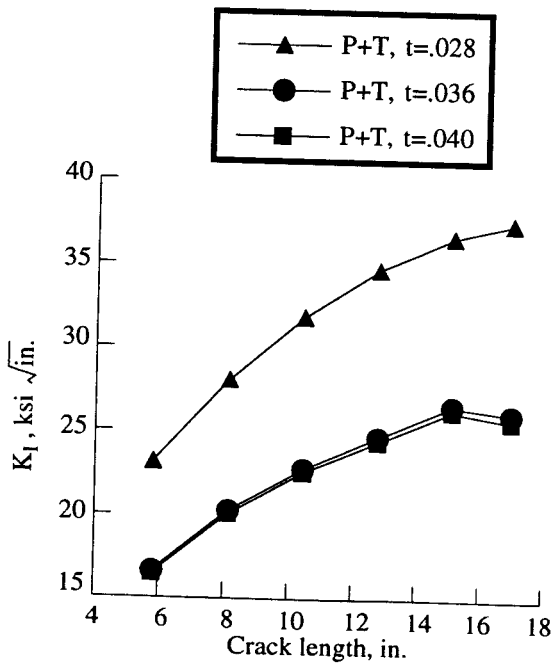
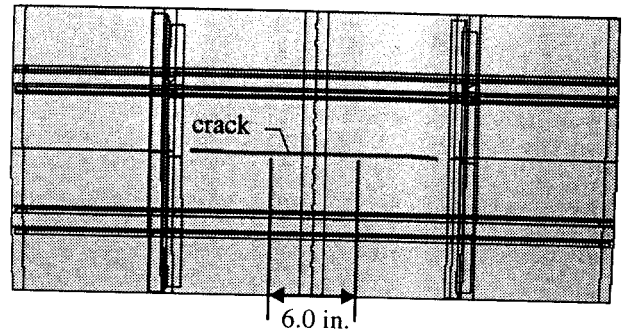
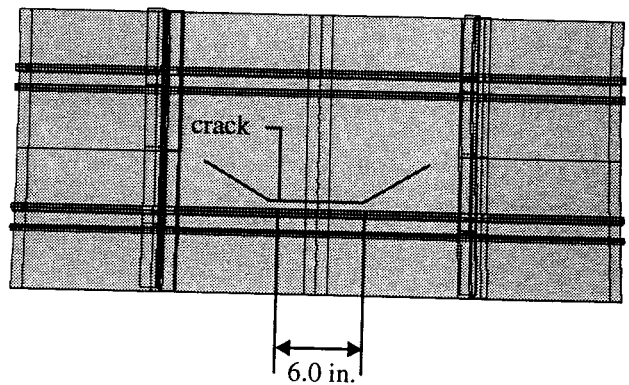


Fig. 7 Effects of varying stiffener thickness on the K_I stress-intensity factor for a six-bay by six-bay stiffened fuselage crown panel with a 17.7 inch-long circumferential crack and subjected to internal pressure and torsion loads.



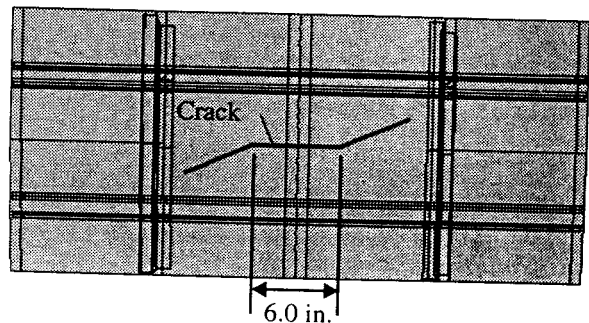
(a) 16-inch-long crack trajectory for internal pressure, bending and vertical shear loads with crack midway between two stringers.

Fig. 8 Crack growth trajectories for a two-bay by three-bay stiffened fuselage crown panel with a 6.0 inch-long initial crack.



(b) 16-inch-long crack trajectory for internal pressure, bending and vertical shear loads with crack 1.2 inches from a stringer.

Fig. 8 Continued.



(c) 16-inch-long crack trajectory for internal pressure and torsion loads with crack initially midway between two stringers.

Fig. 8 Concluded.